L-H transition dynamics in fluid turbulence simulations with neoclassical force balance

L. Chôné[1,2], P. Beyer[1], Y. Sarazin[2], G. Fuhr[1], C. Bourdelle[2], S. Benkadda[1]

[1] *Aix–Marseille Université, CNRS, PIIM UMR 7345, 13397 Marseille Cedex 20, France*

[2] *CEA, IRFM, F-13108 Saint-Paul-lez-Durance, France*

The transition to the high confinement regime, or L-H transition, can occur spontaneously in toroidal magnetic fusion machines when externally injecting power into the plasma [1] and is generally followed by quasi-periodic relaxations of the barrier called Edge-Localised Modes (ELMs) [2]. Since the profits of H-mode can be counterbalanced by the harmful nature of ELMs, thorough understanding of the phenomenon is desirable, but remains shallow for the theoretical part [3, 4]. In particular, plasma edge turbulence simulations based on first principles show self-generation of sheared flows and subsequent turbulence reduction, but no clear transition is observed [4].

Here the non-linear evolution of electrostatic resistive ballooning turbulence in 3D toroidal geometry is described with the following reduced MHD model, in the limit of large aspect ratios and with the slab approximation:

$$\partial_t \nabla_\perp^2 \phi + \left\{\phi, \nabla_\perp^2 \phi\right\} = -\nabla_\parallel^2 \phi - \mathbf{G} p + \nu_\perp \nabla_\perp^4 \phi + \partial_x F_{neo} \quad (1)$$

$$\partial_t p + \{\phi, p\} = \delta_c \mathbf{G} \phi + \chi_\parallel \nabla_\parallel^2 p + \chi_\perp \nabla_\perp^2 p + S(x) \quad (2)$$

With the two fields ϕ and p being respectively the electrostatic potential and the total pressure. Time is here normalised to the interchange time $\tau = \frac{\sqrt{R_0 L_p}}{\sqrt{2}\bar{c}_{S0}}$, the perpendicular length scale is the resistive ballooning length $\xi = \sqrt{\frac{m_i n_0 \eta}{\tau} \frac{L_\parallel}{B_0}}$. The fields are normalised respectively to $\frac{B_0 \xi^2}{\tau}$ and $\frac{\xi p_0}{L_p}$, with L_p the characteristic length of pressure gradient. $\nabla_{\parallel,\perp}$ are the parallel/perpendicular gradient and $\mathbf{G}$ is a toroidal curvature operator. In eq.(2), $\chi_\parallel$ and $\chi_\perp$ account for the parallel and perpendicular collisional heat diffusivities, while in eq.(1), one finds the classical viscosity $\nu_\perp$. A term accounting for neoclassical friction between trapped and circulating particles is added in the model: $F_{neo} = -\mu_{neo}\left(\partial_x \bar{\phi} - K_{neo} \partial_x \bar{p}\right)$, where $\bar{f}$ represents the axisymmetrical part of the field $f = \bar{f} + \tilde{f}$, with $\tilde{f}$ the corresponding perturbation. This term is derived using the radial force balance equation [5, 6]:

$$\partial_r \bar{\phi} + \frac{\partial_r \bar{p}}{en} + \left(\bar{u}_{i,\varphi} B_\theta - \bar{u}_{i,\theta}^{neo} B_\varphi\right) = 0 \quad (3)$$

The toroidal velocity is then assumed small in the absence of torque injection, $B_\varphi \approx B_0$ in the large aspect ratio limit. The neoclassical poloidal velocity is given by: $\bar{u}_{i,\theta}^{neo} = K\left(\nu_{i,*}\right) \frac{\partial_r \bar{T}_i}{eB_0}$ [5, 6], with $K(\nu_{i,*})$ comprised between -2.1 in the Pfirsch-Schlüter regime and 1.17 in the banana regime. Since our model only accounts for the total pressure, neither for density nor temperatures, additional hypotheses are needed for introducing a self-consistent friction term: a fixed ratio between the temperatures $T_i = \varepsilon_T T_e$ is assumed, as well as a constant density so the ion temperature gradient can be written in terms of total pressure. $K(\nu_{i,*})$ and μ_{neo} are determined using approximate fits that can be found respectively in [5] and [7]. This last point is motivated by the strong variations of μ_{neo} and K_{neo} at the edge, and by the fact that no transport barrier was triggered during preliminary simulations using constant coefficients.

The MHD model can be further simplified by considering the flute approximation $k_{\parallel} = 0$ and retaining only one poloidal mode of wavenumber k, resulting in the following 1D system [8]:

$$\partial_t \bar{p} = -\imath k \partial_x \left(\tilde{p}\tilde{\phi}^* - \tilde{p}^*\tilde{\phi}\right) + \chi_{\perp}\partial_x^2 \bar{p} + S \quad (4)$$

$$\partial_t \bar{V} = \imath k \partial_x \left(\tilde{\phi}\partial_x\tilde{\phi}^* - \tilde{\phi}^*\partial_x\tilde{\phi}\right) - \mu_{neo}\left(\bar{V} - K_{neo}\partial_x\bar{p}\right) + \nu_{\perp}\partial_x^2 \bar{V} \quad (5)$$

$$\partial_t \tilde{p} = \imath k \left[\tilde{\phi}\left(\partial_x \bar{p} - \kappa\right) - \bar{V}\tilde{\phi}\right] - \alpha_p \left|\tilde{p}\right|^2 \tilde{p} + \chi_{\perp}\partial_x^2 \tilde{p} \quad (6)$$

$$\partial_t \tilde{\phi} = \imath \left(\frac{g}{k}\frac{\tilde{p}}{\bar{p}} - k\bar{V}\tilde{\phi}\right) - \alpha_\phi \left|\tilde{\phi}\right|^2 \tilde{\phi} + \nu_{\perp}\partial_x^2 \tilde{\phi} \quad (7)$$

With the equilibrium poloidal velocity $\bar{V} = \partial_x \bar{\phi}$. The $\alpha_f \left|\tilde{f}\right|^2 \tilde{f}$ terms account for saturation via mode coupling. Here t is normalised by $\frac{1}{\omega_S} = \frac{m_i}{eB_0}$, x by $\rho_S = \frac{\sqrt{m_i k_B T_e}}{eB_0}$. $L_p = \rho_S$.

3D simulations are carried out using the EMEDGE3D code [9]. The simulation domain corresponds roughly to $0.85 < \rho < 1$ and is bounded by buffer zones where the turbulence is artificially stabilised by large $\chi_{\perp}$ and $\nu_{\perp}$. All simulations are flux-driven by a source $S(x)$ located in the $x < x_{min}$ buffer zone, with the amplitude $S_0 = \int S(x)\,dx$. The safety factor is hyperbolic, between $q(x_{min}) = 2.5$ and $q(x_{max}) = 3.5$.

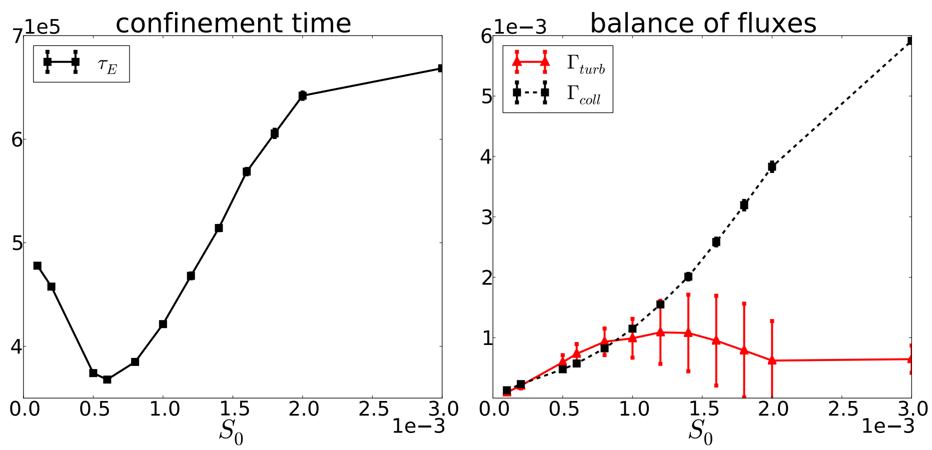

Figure 1: Evolution of the confinement efficiency as a function of the heat source amplitude in the 1D case.

In the 1D case, partial stabilisation of the turbulence is achieved above a certain threshold of the injected power, as shown on Figure 1. In the parameter range considered so far, it turns out that the collisional and turbulent fluxes are of the same order of magnitude (Figure 1, right panel). The main interest of these results resides in the dynamics of the system once the turbulence level is strongly reduced: here turbulence is not completely suppressed but shows instead quasi-periodic bursts. Interestingly the pseudo-period increases with the injected power (see Figure 2). This behaviour bears similarities with type-III ELMs, which were shown to be governed by the resistive ballooning instability [10].

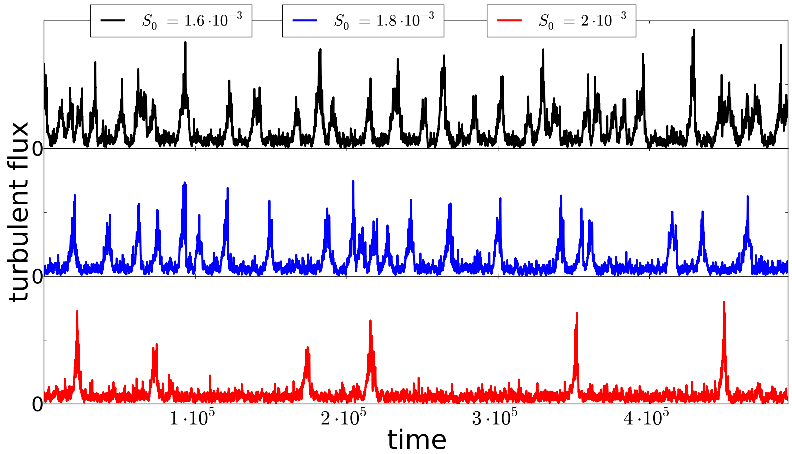

Figure 2: Time evolution of the turbulent flux at the position of the barrier for different heat source amplitudes in the 1D case. The y-axis of the three curves are at the same scale.

Since the 1D model naturally offers a simpler picture of the phenomenon, let us now consider the 3D model. Here the parameters are chosen close to the experiment, corresponding to the geometry of a TEXTOR-like machine. This is with the exception of $\nu_\perp$ and $\chi_\perp$, chosen large enough so as to ensure damping at sub-Larmor scales. When increasing the neoclassical friction coefficient μ_{neo}, above a certain threshold, a transport barrier is generated at the edge. Here, apart from the region where the barrier exists, the collisional flux is very small compared to the turbulent flux, in agreement with experimental conditions. The reduction of the turbulent flux observed at the barrier position is caused by the generation of a strongly sheared radial electric field when the friction term becomes dominant. Although the scrape-off layer physics is not included in the model, its radial profile shows the well characteristic of H-mode (see Figure 3, right panel) and is in good qualitative agreement with experimental measurements [11]. It is also observed that the location of the barrier is governed by the local neoclassical regime, more precisely at the transition from Pfirsch-Schlüter to plateau regime, where the gradient of K_{neo} is the strongest. This position coincides with a maximum of μ_{neo}, i.e. a maximum of the friction effect. Notice also that no relaxations of the barrier were observed yet in the 3D case.

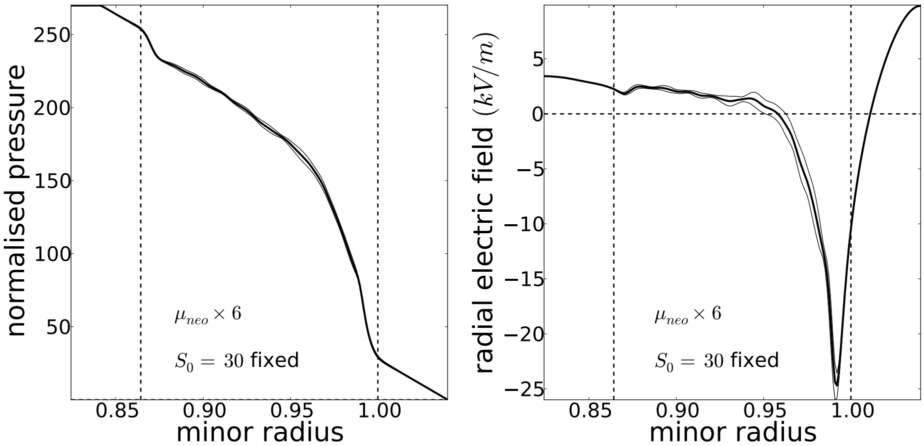

Figure 3: Pressure and radial electric field profile showing a barrier in the 3D case. The fine solid lines show the standard deviation to the mean profile, the vertical dashed lines are the boundaries between the main simulation domain and the buffer zones.

In conclusion, we have shown, by means of both 1D and 3D models for edge turbulence, that allowing relaxation of the poloidal flow towards a self-consistent neoclassical value can generate a transport barrier associated with a strong sheared flow. Its characteristics are in good agreement with experimental measurements in the 3D case. Furthermore, while the 1D model useholds strong simplifications, it shows that the shear associated with neoclassical rotation increases with the injected power leading to less frequent bursts. This corresponds to experimental observations for type-III ELMs [2], which can be described by the sole resistive ballooning instability [10], as opposed to type-I ELMs which are governed by the peeling-ballooning instability [2]. This work has been supported by the French National Research Agency, project ANR-2010-BLAN-940-01.

References

[1] F. Wagner, G. Becker, K. Behringer *et.al*, Phys. Rev. Lett. **49**, 1048 (1982).
[2] H. R. Wilson, S. C. Cowley, A. Kirk, P. B. Snyder, Plasma Phys. Control. Fusion **48**, (2006) A71–A84.
[3] J. W. Connor, H. R. Wilson, Plasma Phys. Control. Fusion **42** (2000) R1–R74.
[4] J. W. Connor, "Recent Progress in the Theoretical Modelling of the L-H Transition", 17th Joint EU-US Transport Task Force Meeting, Padua, Septembre 3-6, 2012.
[5] F. L. Hinton, R. D. Hazeltine, Rev. Mod. Phys. **48**, 239 (1976).
[6] P. Helander, D. J. Sigmar, Collisional Transport in Magnetized Plasmas, Cambridge University Press (2005).
[7] T. A. Gianakon, S. E. Kruger, and C. C. Hegna, Phys. Plasmas **9**, 536 (2002).
[8] S. Benkadda *et.al*, Nucl. Fusion **41** (2001) 995.
[9] G. Fuhr, P. Beyer, and S. Benkadda, Phys. Rev. Lett. **101**, 195001 (2008).
[10] P. Beyer *et.al* , Phys. Rev. Lett. **94**, 105001 (2005).
[11] E. Viezzer, T. Pütterich, G.D. Conway *et.al*, Nucl. Fusion **53** (2013) 053005.